

# Direct Modeling of Envelope Dynamics in Resonant Inverters

Yan Yin, Regan Zane, Robert Erickson  
Colorado Power Electronics Center  
University of Colorado at Boulder  
Boulder, CO 80309-0425

John Glaser  
General Electric Company  
Global Research Center  
One Research Circle  
Niskayuna, NY 12309

**Abstract**— This paper provides a direct dynamic modeling approach for envelope signals in resonant inverters driven by modulated inputs (AM or FM). Based on the sinusoidal approximation, this approach decomposes the modulated input into its fundamental component plus two dominant sidebands. The system response is then found by the summation of the responses to the three individual inputs. Following this conception, the small signal transfer functions for envelope signals in a resonant inverter are then derived. Some simple but useful results for these transfer functions are presented, which link the transfer functions of envelope signals to the transfer functions of the resonant tank and simplify hand calculations. This modeling approach is verified with simulation and experimental results by studying the dynamic responses of output current envelope to bus voltage and switching frequency.

## I. INTRODUCTION

High-frequency dc-to-ac inverters are used in a variety of applications including electronic ballasts for discharge lamps, induction heating, and medical devices. The dc power input is generally converted to a high frequency ac output through use of a switch network followed by a resonant tank, as illustrated in Fig. 1. The output power can then be regulated by controlling the bus voltage and/or the switching frequency. This is due to the frequency dependant nature of the resonant tank, where input variations in both the bus voltage (amplitude modulation, AM) and the switching frequency (frequency modulation, FM) result in amplitude variations at the load. Thus the objective of the controller is to regulate the envelope or magnitude of the signals at the load. A common objective with a long history is to model the ac dynamics from input modulation to output envelopes in order to facilitate optimized controller design. Several approaches are available to model the envelope dynamics of a resonant inverter. The lumped parameter equivalent circuit model in [1] was obtained by considering the resonant converter as a sampled-data nonlinear system. But the results are too complicated to provide good intuitive insight into the system operation. A generalized averaging approach was proposed in [2], which is based on a time-dependent Fourier series representation of a periodic waveform. Simplified approximation can be made by ignoring insignificant terms in the series and only retaining the dominant components. This is especially true for high-Q resonant circuits, where the fundamental component is of interest. Based on a similar concept, a phasor transformation approach was proposed in [3] and applied to study the dynamics of resonant ballasts in [4-6]. The time-varying phasor in [3-6] is essentially

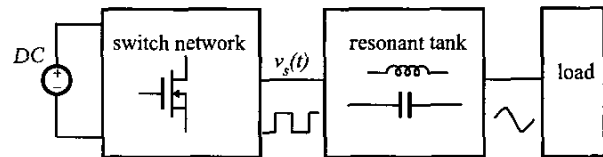


Fig. 1 General configuration for a resonant inverter

equivalent to the complex coefficient of the fundamental component in the Fourier series. The describing function is another approach that decomposes the modulated waveforms into sine and cosine waveforms, and the small-signal model is obtained by performing harmonic approximation and balance as in [7]. However, to some extent, the approaches in [2-7] are based on the transformation of the original resonant tank, and the physical meaning of the system responses to modulated inputs is partly lost during the transformation.

Another possible approach is to decompose the modulated input (AM or FM) into three dominant components: its fundamental component plus two sidebands. The overall response of the linear system to the modulated input is considered as the summation of the responses to the three individual inputs. Then the small signal transfer functions from bus voltage/switching frequency to output envelopes can be obtained. This approach was used in [8,9] to analyze the envelope dynamics of the resonant tank in  $s$ -domain at a fixed frequency with controllable reactive elements. Still lacking is a general result to reveal the inherent relationship between the envelope dynamics and the tank dynamics. In this paper, we provide general expressions to model the dynamic responses of signal envelopes in a resonant inverter system to bus voltage variations (AM) as well as switching frequency variations (FM). Compared with previous results in [1-9], the final transfer functions we obtain through this approach retain a strong physical relationship to the transfer function of the original resonant tank. Our results also confirm mathematically the intuitive results discussed in [10] with respect to low-frequency pole positions.

In Section II, the general decompositions for AM and FM inputs are presented. Step-by-step derivations of the small-signal transfer functions are then presented in Section III. Section IV highlights some insightful results that are useful for design-oriented analysis. The theoretical analysis is then verified by simulation and experimental results in Section V. Our conclusions are provided in Section VI.

## II. DECOMPOSITION OF MODULATED INPUTS

The spectrum of the square-wave  $v_s(t)$  in Fig. 1 contains a fundamental ac component as well as higher-order harmonics. If the switching frequency is close to the resonant frequency  $f_0$  and the tank has high  $Q$ -factor, then the higher-order harmonics of  $v_s(t)$  will be filtered by the resonant tank such that the load current and voltage are essentially sinusoidal with frequency  $f_s$ . Hence the sinusoidal approximation can be applied, which greatly simplifies the analysis [11]. For the half-bridge switching network,  $v_s(t)$  can be approximately expressed as

$$v_s(t) \approx \frac{2}{\pi} V_g \cos(2\pi f_s t), \quad (1)$$

where  $V_g$  is the bus voltage and  $f_s$  is the switching frequency. Then if there are small variations in the bus voltage or switching frequency, the input to the resonant tank behaves similar to a sinusoidal signal with amplitude or frequency modulation.

In general, a modulated sinusoidal signal can be expressed as the sum of a series of signals with frequencies  $f_s$ ,  $f_s + f_m$ ,  $f_s - f_m$ ,  $f_s + 2f_m$ ,  $f_s - 2f_m$ , etc, where  $f_s$  is the carrier frequency and  $f_m$  is the modulating frequency. If the magnitude of the modulating signal is very small compared to the carrier signal (narrow-band modulation for FM [12]), then the modulated input can be simplified as the sum of three dominant components with frequencies  $f_s$ ,  $f_s + f_m$ ,  $f_s - f_m$ , where the magnitude of the fundamental component at  $f_s$  is much larger than the two sidebands, as shown in Fig. 2.

Based on these assumptions, we can decompose the modulated inputs to the resonant tank into three individual inputs, as shown below for AM and FM.

AM inputs in form of

$$v_{s\_AM}(t) = \frac{2}{\pi} [V_g + c_v \cos(\omega_m t)] \cos(\omega_s t), \quad c_v < V_g \quad (2)$$

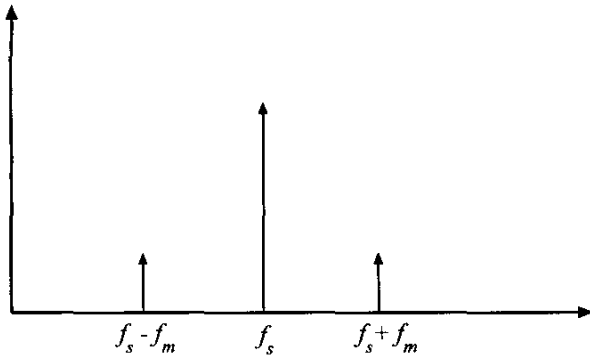


Fig.2 Spectrum of a modulated signal with small modulation

are approximately expressed as

$$v_{s\_AM}(t) = \frac{2}{\pi} \left\{ V_g \cos(\omega_s t) + \frac{c_v}{2} \cos[(\omega_s + \omega_m)t] + \frac{c_v}{2} \cos[(\omega_s - \omega_m)t] \right\}, \quad (3)$$

where  $\omega_s = 2\pi f_s$ ,  $\omega_m = 2\pi f_m$ .

Similarly, narrow-band FM inputs in form of

$$v_{s\_FM}(t) = \frac{2}{\pi} V_g \cos[\omega_s t + \int c_\omega \cos(\omega_m t) dt], \quad (4)$$

$$c_\omega \ll \omega_s \text{ and } \frac{c_\omega}{\omega_m} \ll \pi/2$$

are approximately expressed as

$$v_{s\_FM}(t) = \frac{2V_g}{\pi} \left\{ \cos(\omega_s t) + \frac{c_\omega}{2\omega_m} \cos[(\omega_s + \omega_m)t] - \frac{c_\omega}{2\omega_m} \cos[(\omega_s - \omega_m)t] \right\}. \quad (5)$$

Equations (3) and (5) are the desired results, which explicitly express the AM and FM inputs in three individual inputs with frequencies  $\omega_s$ ,  $\omega_s + \omega_m$ ,  $\omega_s - \omega_m$ , respectively.

## III. DERIVATION OF SMALL-SIGNAL TRANSFER FUNCTIONS FOR OUTPUT ENVELOPES IN RESONANT INVERTERS

As the modulated inputs (AM or FM) have been decomposed into three sinusoidal inputs, then the output of the inverter (which is a linear network) can be considered as the summation of the network responses to the three inputs. In the following, we use FM input as an example to derive the small-signal transfer function from frequency to output envelope. A similar procedure can also be applied for AM inputs, while only the results are presented here.

From (5), the frequency domain transformation of the FM inputs can be written as

$$V_{s\_FM}(j\omega) = \frac{2V_g}{\pi} \left\{ \pi[\delta(\omega - \omega_s) + \delta(\omega + \omega_s)] - \frac{1}{2\omega_m} \pi[\delta(\omega - (\omega_s - \omega_m)) + \delta(\omega + (\omega_s - \omega_m))] + \frac{1}{2\omega_m} \pi[\delta(\omega - (\omega_s + \omega_m)) + \delta(\omega + (\omega_s + \omega_m))] \right\}. \quad (6)$$

For simplicity,  $c_\omega$  in (5) has been set to be unity. Then the system response in the frequency domain can be easily written as

$$X_{out}(j\omega) = V_{s\_FM}(j\omega) G(j\omega), \quad (7)$$

where  $X_{out}(j\omega)$  represents the frequency response of any output and  $G(j\omega)$  is the bus voltage-to-output transfer function, which can be found easily using standard analysis techniques [11]. The reverse transformation of  $X_{out}(j\omega)$  leads to

$$x_{out}(t) = \frac{2V_g}{\pi} \|A\| \cos(\omega_s t + \angle A), \quad (8)$$

where

$$\begin{aligned} A &= A_0 + A_l e^{-j\omega_s t} + A_u e^{j\omega_s t} \\ A_0 &= G(j\omega_s) \\ A_l &= -\frac{1}{2\omega_m} G[j(\omega_s - \omega_m)] \\ A_u &= \frac{1}{2\omega_m} G[j(\omega_s + \omega_m)]. \end{aligned} \quad (9)$$

Hence, the expression for the output envelope is obtained, which is equal to  $\frac{2V_g}{\pi} \|A\|$ .  $A_0$ ,  $A_l$ , and  $A_u$  in (9) represent the tank responses to the fundamental component, lower sideband, and upper sideband, respectively.

Next we need to extract the small-signal portion of  $\|A\|$ , which will be the desired transfer function from frequency to output envelope (because we have set the magnitude of frequency variation,  $c_\omega$ , to be unity and the phase of frequency variation to be zero). We note that

$$\begin{aligned} \|A\|^2 &= AA^* \\ &= (A_0 + A_l e^{-j\omega_s t} + A_u e^{j\omega_s t})(A_0^* + A_l^* e^{j\omega_s t} + A_u^* e^{-j\omega_s t}) \\ &= \|A_0\|^2 + \|A_l\|^2 + \|A_u\|^2 \\ &\quad + 2\|A_0 A_l^* + A_0^* A_u\| \cos[\omega_m t + \angle(A_0 A_l^* + A_0^* A_u)] \\ &\quad + 2\|A_l^* A_u\| \cos[2\omega_m t + \angle(A_l^* A_u)], \end{aligned} \quad (10)$$

where “\*” represents complex conjugate. For small variations in the switching frequency, we can apply the small-signal assumption  $\|A_l\|, \|A_u\| \ll \|A_0\|$  and neglect  $\|A_l\|^2$  and  $\|A_u\|^2$  as well as the component with  $2\omega_m$ , which leads

$$\|A\|^2 \approx \|A_0\|^2 + 2\|A_0 A_l^* + A_0^* A_u\| \cos[\omega_m t + \angle(A_0 A_l^* + A_0^* A_u)]. \quad (11)$$

By taking the square root and linearizing  $\|A\|$ , we obtain

$$\begin{aligned} \|A\| &\approx \|A_0\| \\ &\quad + \frac{\|A_0 A_l^* + A_0^* A_u\|}{\|A_0\|} \cos[\omega_m t + \angle(A_0 A_l^* + A_0^* A_u)]. \end{aligned} \quad (12)$$

Equation (12) explicitly expresses  $\|A\|$  as a dc component  $\|A_0\|$  plus an ac component. The dc component, which is defined as  $G(j\omega_s)$ , represents the steady-state response of  $x_{out}(t)$  at the switching frequency, while the ac component models small variations in the envelope caused by frequency modulation. The magnitude and phase of the ac component correspond to the magnitude and phase of the small-signal transfer function from frequency to output envelope. Combining the magnitude and phase expressions, one obtains the transfer function of control to output envelope as

$$G_{\omega\_en}(j\omega_m) = \frac{2V_g}{\pi} \frac{A_0 A_l^* + A_0^* A_u}{\|A_0\|}, \quad (13)$$

where  $A_0$ ,  $A_l$ ,  $A_u$  are defined in (9).

Following similar steps, we can solve for the effects of AM to derive the transfer function from line to output envelope. It has a similar expression as (13), given by

$$G_{v\_en}(j\omega_m) = \frac{2}{\pi} \frac{A_0 A_l^* + A_0^* A_u}{\|A_0\|} \quad (14)$$

with  $A_0$ ,  $A_l$ ,  $A_u$  defined as follows

$$\begin{aligned} A_0 &= V_g G(j\omega_s) \\ A_l &= \frac{1}{2} G[j(\omega_s - \omega_m)] \\ A_u &= \frac{1}{2} G[j(\omega_s + \omega_m)]. \end{aligned} \quad (15)$$

Equations (13) and (14) are the desired results, which explicitly relate the envelope transfer functions to the transfer function of the original tank and reveal the inherent relationship between the envelope transfer functions and the resonant tank transfer functions. The envelope dynamics at the modulating frequency  $\omega_m$  are then modeled by the responses to two sidebands defined as  $A_l$  and  $A_u$ . It should be noted that although the coefficients of  $A_l$  and  $A_u$  in (9) and (15) are complex, the coefficients of (13) and (14) are still real when we take  $j\omega_m$  as the variable. The proof is provided in the appendix

#### IV. DISCUSSIONS

By putting (13) and (14) into mathematic tools such as Matlab, we can get detailed information for the target transfer functions. To facilitate hand calculations, we highlight a couple of simple but useful results for these transfer functions. In the following discussion, we assume the transfer function of the resonant tank is in form of

$$G(j\omega) = \frac{N(j\omega)}{D(j\omega)} = \frac{N_1(\omega) + jN_2(\omega)}{D_1(\omega) + jD_2(\omega)}. \quad (16)$$

##### A. Poles

By substituting (16) into the transfer function defined in (14) & (15), the denominator can be generally expressed as

$$D_{v\_en}(j\omega_m) = D(j\omega_m + j\omega_s)D(j\omega_m - j\omega_s). \quad (17)$$

Equation (13) is a little different from (14) because  $A_l$  and  $A_u$  contain “ $1/\omega_m$ ”, which means the denominator will be in form of

$$D_{\omega\_en}(j\omega_m) = \omega_m D(j\omega_m + j\omega_s)D(j\omega_m - j\omega_s). \quad (18)$$

However, it can be shown that  $\omega_m$  in the denominator will be cancelled by the numerator (see appendix for the proof), so the denominator of (13) still has the same form as (17). From (17), it is clear that poles of (13) and (14) can be obtained by

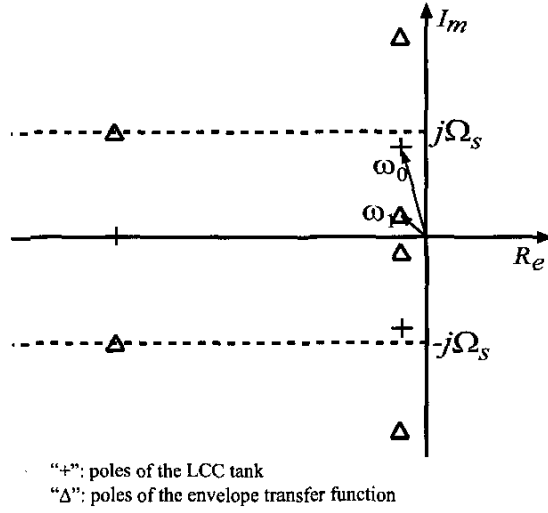


Fig 3 Relationship between poles of a LCC tank and its envelope transfer function

shifting the poles of resonant tank up and down in the  $s$ -domain by  $j\omega_s$ . The relationship between the poles of the envelope transfer functions and the poles of the resonant tank for a typical LCC inverter is shown in Fig. 3. For most applications, there is a pair of low-frequency poles with frequency  $\omega_1$  as

$$\omega_1 = \sqrt{\omega_s^2 - 2\omega_s\omega_0\sqrt{1-1/(4Q^2)} + \omega_0^2} \approx |\omega_s - \omega_0| \text{ for high } Q, \quad (19)$$

where  $\omega_0$  and  $Q$  are resonant frequency and quality factor of the resonant tank. This result is the same as the one obtained with phasor transformation approach in [3] and also in agreement with the approximation made in [10], where it is obtained based on physical understandings of the resonant tank operation.

### B. DC gains

The DC gains of (12) and (13) can also be found by only evaluating the transfer functions of the original tank, which have been extensively studied in [11].

For (13), by setting  $\omega_m$  to zero, the DC gain can be manipulated into the following form

$$G_{0-\omega} = \frac{2V_g}{\pi} \frac{N_{0-\omega}}{D_{0-\omega}}, \quad (20)$$

where

$$D_{0-\omega} = \sqrt{D_1^2(\omega_s) + D_2^2(\omega_s)} \sqrt{N_1^2(\omega_s) + N_2^2(\omega_s)} [D_1^2(\omega_s) + D_2^2(\omega_s)]$$

$$N_{0-\omega} = [D_1^2(\omega_s) + D_2^2(\omega_s)] [N_1(\omega_s) \frac{\partial N_1(\omega_s)}{\partial \omega_s} + N_2(\omega_s) \frac{\partial N_2(\omega_s)}{\partial \omega_s}]$$

$$- [N_1^2(\omega_s) + N_2^2(\omega_s)] [D_1(\omega_s) \frac{\partial D_1(\omega_s)}{\partial \omega_s} + D_2(\omega_s) \frac{\partial D_2(\omega_s)}{\partial \omega_s}]. \quad (21)$$

Equation (20) is equivalent to differentiating the magnitude of (16) with frequency and evaluating it at  $\omega_s$  as

$$G_{0-\omega} = \frac{2V_g}{\pi} \frac{\partial \|G(j\omega)\|}{\partial \omega} \Big|_{\omega=\omega_s}. \quad (22)$$

For (14), the DC gain can also be easily obtained by setting  $\omega_m$  to zero, resulting in the simple expression

$$G_{0-v} = \frac{2}{\pi} \|G(j\omega_s)\|. \quad (23)$$

We do not have a general form for zeroes that can be applied to all resonant inverters. The zeroes can only be evaluated for a given tank. However, as long as the zeroes are well above the switching frequency, these simple results about poles and dc gain can be conveniently used to predict the dominant low-frequency envelope dynamics of the system based only on evaluation of the original resonant tank, which boosts our physical understanding of the system operation and facilitates closed-loop controller design.

## V. MODEL VERIFICATION

In this section, the LCC resonant inverter as shown in Fig. 4 is studied, and the theoretical results derived in Section III are verified by examining the envelope dynamics of output current  $i_{out}$  with the network response given by

$$G(j\omega) = \frac{i_{out}(j\omega)}{v_s(j\omega)} = \frac{j\omega C_s}{1 + j\omega C_s R + (j\omega)^2 L(C_s + C_p) + (j\omega)^3 L C_s C_p R}. \quad (24)$$

Figure 5 and Fig. 6 compare the simulation results of the envelope signals with the resonant waveforms for AM/FM inputs. The envelope signals are plotted by evaluating (13) and (14) at  $V_g = 155$  V,  $f_s = 100$  kHz and  $f_m = 1$  kHz with  $c_v = 10$  V and  $c_\omega = 2\pi * 500$  rad/s. For comparison the resonant waveforms are obtained by solving the differential equations of the LCC tank with the same AM/FM inputs. It can be seen that (13) and (14) give the envelope waveforms

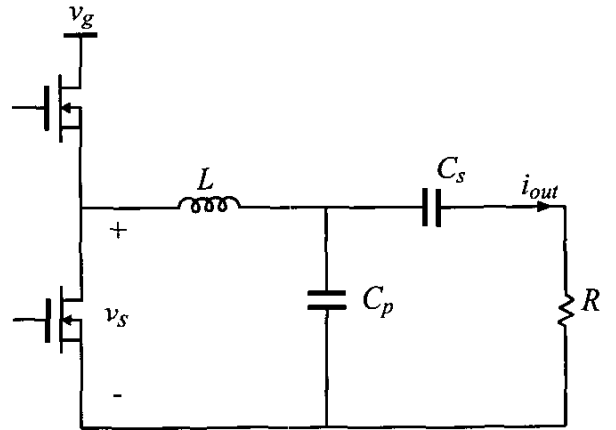


Fig. 4 LCC inverter  $L=539\mu\text{H}$ ,  $C_s=4.3\text{nF}$ ,  $C_p=3.8\text{nF}$   $R=300\Omega$

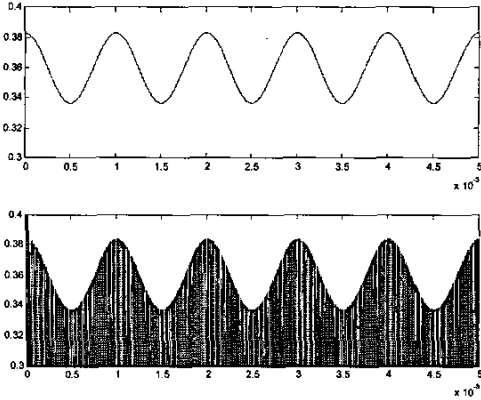


Fig.5 Comparison of time-domain simulation waveforms for AM input (top: envelope signal, bottom: resonant waveform)

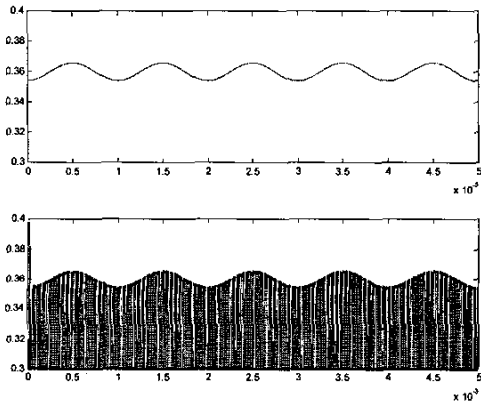


Fig 6 Comparison of time-domain simulation waveforms for FM input (top: envelope signal; bottom: resonant waveform)

of the resonant tank without requiring complete switching-frequency level solutions.

Figure 7 and Fig. 8 compare the transfer functions from bus voltage to output current envelope and switching frequency to output current envelope for the same LCC inverter shown in Fig. 4. The agreements between theoretical and experimental results are quite good. The resonant frequency for the studied LCC inverter is 80kHz, and the steady-state switching frequency is 100kHz. Hence according to (19), the approximate value for the low-frequency double pole is 20kHz, which is in agreement with the measurements.

## VI. CONCLUSIONS

In this paper, we provide a direct approach to model the dynamics of envelope signals in resonant converters. This approach is based on the sinusoidal approximation and decomposes the modulated inputs (AM or FM) into three sinusoidal inputs. The system response to the modulated input is then considered as the summation of the responses to

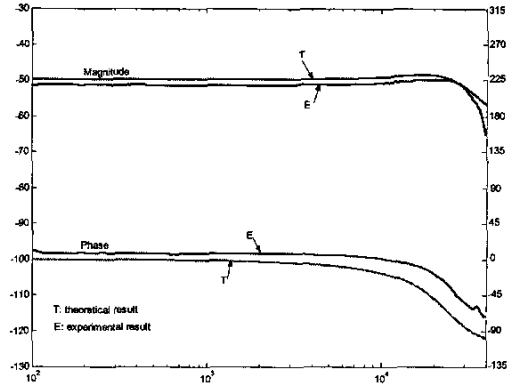


Fig.7 Comparison between theoretical and experimental results for bus voltage-to-output current envelope transfer function

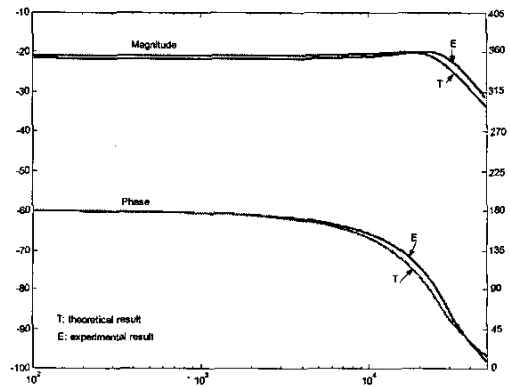


Fig.8 Comparison between theoretical and experimental results for frequency-to-output current envelope transfer function

the three inputs. Based on this concept, the theoretical results for the small signal transfer functions of envelope signals are derived, which reveal the inherent relationship between the dynamics of the envelopes and those of the resonant tanks. Some simple but useful results for these transfer functions are obtained, which can facilitate hand calculations of the transfer functions directly from the characteristics of the original resonant tank. The theoretical results are verified by simulations and experiments.

## APPENDIX

For frequency modulation, the denominator for the envelope transfer function (13) will be in form of (18). In the following, the detailed proof is provided to show that in (18)  $\omega_m$  will be canceled by the numerator such that the denominator of (13) still has the same form as (17), which is in agreement with basic linear system theory. We also show that the transfer functions (13) and (14) have real coefficients.

Assuming the resonant tank transfer function is defined as (16), we can get the general expression for the numerator of (13) by substituting (16) into (13)

$$\begin{aligned} N_{\omega_{en}}(j\omega_m) &= N(j\omega_s)N(j\omega_m - j\omega_s)D(-j\omega_s)D(j\omega_m + j\omega_s) \\ &\quad - N(-j\omega_s)N(j\omega_m + j\omega_s)D(j\omega_s)D(j\omega_m - j\omega_s) \\ &= N_1(j\omega_m) - N_2(j\omega_m), \end{aligned} \quad (25)$$

where

$$\begin{aligned} N_1(j\omega_m) &= N(j\omega_s)N(j\omega_m - j\omega_s)D(-j\omega_s)D(j\omega_m + j\omega_s) \\ N_2(j\omega_m) &= N(-j\omega_s)N(j\omega_m + j\omega_s)D(j\omega_s)D(j\omega_m - j\omega_s). \end{aligned}$$

The objective is to prove that (25) can be manipulated into the form as

$$N_{\omega_{en}}(j\omega_m) = \omega_m P(j\omega_m), \quad (26)$$

where  $P(j\omega_m)$  is a polynomial with real coefficients. In other words, it should be proven that (25) has no any term independent of  $\omega_m$ .

For a linear system, both  $N(j\omega)$  and  $D(j\omega)$  are polynomials. The terms in  $N_1(j\omega_m)$  independent of  $\omega_m$  can be expressed as

$$N(j\omega_s)N(-j\omega_s)D(-j\omega_s)D(j\omega_s). \quad (27)$$

It is clear that (27) also holds true for  $N_2(j\omega_m)$ . Hence the terms independent of  $\omega_m$  in  $N_1(j\omega_m)$  and  $N_2(j\omega_m)$  will be cancelled due to the “-” sign in (25).

Then all the remaining terms in  $N_{\omega_{en}}(j\omega_m)$  can be generally expressed as

$$k \bullet (j\omega_s)^p (j\omega_m)^q, \quad (28)$$

where  $q \geq 1$ . It can also be proven that the index  $p$  in (28) is odd (see below), then (28) can be further manipulated into a form as

$$\omega_m \bullet k \bullet j^{p+1} \omega_s^p (j\omega_m)^{q-1}. \quad (29)$$

Given  $p+1$  is even,  $j^{p+1}$  is either 1 or  $-1$ , such that expression (29) can be written as (26). And  $\omega_m$  in (29) will be cancelled by the denominator as (18). Expression (29) also shows that the coefficients of  $N_{\omega_{en}}(j\omega_m)$  are real.

The fact that  $p$  in (28) is odd can be seen by extending  $N_1(j\omega_m)$  of (25) into the sum of a series of terms in form of

$$k_0 \bullet (j\omega_s)^a (j\omega_m - j\omega_s)^b (-j\omega_s)^c (j\omega_m + j\omega_s)^d, \quad (30)$$

where  $a, b, c, d \geq 0$ . By expanding (30), we can express it as the sum of terms in form of

$$k_0 \bullet (j\omega_s)^a C_b^e (j\omega_m)^e (-j\omega_s)^{b-e} (-j\omega_s)^c C_d^f (j\omega_m)^f (j\omega_s)^{d-f}, \quad (31)$$

where  $0 \leq e \leq b$ ,  $0 \leq f \leq d$ . Expression (31) can be more explicitly written as

$$k_0 C_b^e C_d^f (-1)^{b-e+c} (j\omega_s)^{a+b-e+c+d-f} (j\omega_m)^{e+f}. \quad (32)$$

Similarly,  $N_2(j\omega_m)$  can be written as the sum of terms as

$$k_0 C_b^e C_d^f (-1)^{a+d-f} (j\omega_s)^{a+b-e+c+d-f} (j\omega_m)^{e+f}. \quad (33)$$

By comparing (32) and (33), we can find that if the index  $a+b-e+c+d-f$ , which is equivalent to  $p$  in (28), is even, then both  $b-e+c$  and  $a+d-f$  should be either even or odd, which means (32) and (33) are equal and will be cancelled due to the “-” sign in (25). Then the final expression of  $N_{\omega_{en}}(j\omega_m)$  will only contain those terms in form of (28) while  $p$  is odd.

Based on similar argument, it is easy to prove that for amplitude modulation, the numerator of (14) can also be expressed as the sum of items similar to a form as (28) while  $p$  is even. Then  $j^p$  is either 1 or  $-1$ , so the numerator of (14) also has real coefficients.

The denominators of (13) and (14) have the same form as (17). When we take  $j\omega_m$  as the variable,  $D(j\omega_m + j\omega_s)$  and  $D(j\omega_m - j\omega_s)$  are complex conjugates, hence the coefficients of (17) are also real. Such that we get the conclusion that both (13) and (14) are with real coefficients as conventional transfer functions.

## REFERENCES

- [1] A. F. Witulski, A. F. Hernandez, and R. Erickson, “Small Signal Equivalent Circuit Modeling of Resonant Converters,” IEEE Trans. on Power Electronics, Vol. 6, No. 1, January 1991, pp11-27.
- [2] S. R. Sanders, J. M. Noworolski, X. Z. Liu, and G. C. Verghese, “Generalized Averaging Method for Power Conversion Circuits,” IEEE Trans. on Power Electronics, Vol. 6, No.2, April 1991, pp251-259.
- [3] C. T. Rim and G. H. Cho, “Phasor Transformation and its Application to the DC/AC Analyses of Frequency Phase-Controlled Series Resonant Converters (SRC),” IEEE Trans. on Power Electronics, Vol.5, No.2 April 1990, pp 201-211.
- [4] Y. Yin, R. Zane, R. Erickson, and J. Glaser, “Dynamic Analysis of Frequency-Controlled Electronic Ballasts”, IEEE Industry Applications Conference, 37<sup>th</sup> IAS annual meeting, October 2002
- [5] S. Ben-Yaakov, S. Gluzman, and R. Rabinovici, “Envelope Simulation by SPICE-Compatible Models of Linear Electric Circuits Driven by Modulated Signals,” IEEE Trans. on Industry Application, Vol. 37, No.2, March/April 2001, pp 527-533.
- [6] E. Deng, “1. Negative Incremental Impedance of Fluorescent Lamp”, Ph.D. thesis, California Institute of Technology, Pasadena, 1995.
- [7] E. X. Yang, F. C. Lee, and M. M. Jovanovic, “Small-signal Modeling of Series and Parallel Resonant Converters,” Applied Power Electronics Conference and Exposition, 1992, APEC’92 Conference Proceedings, 785-792.
- [8] J. L. Vollin, “Resonant power processing at a fixed frequency using a controllable inductance”, Ph.D. thesis, California Institute of Technology, Pasadena, 1993.
- [9] J.-H. Cheng, A. F. Witulski, and J. L. Vollin, “A Small-Signal Model Utilizing Amplitude Modulation for the Class-D Converter at Fixed Frequency”, IEEE Trans. on Power Electronics, Vol. 15, No. 6, November 2000, pp1204-1211.
- [10] V. Vorperian, “Approximate Small-Signal Analysis of the Series and the Parallel Resonant Converters,” IEEE Trans. on Power Electronics, Vol.4, No.1, January 1989, pp 15-24.
- [11] R. Erickson, D. Maksimovic, *Fundamentals of Power Electronics, second edition*, Massachusetts: Kluwer Academic Publishers, 2000.
- [12] J. D. Gibson, *Principles of Digital and Analog Communications*, New York, Macmillan Publishing Company, 1989.